International Journal of Automotive Technology, Vol. 11, No. 1, pp. 33–40 (2010)
DOI 10.1007/s12239–010–0005–5

1229–9138/2010/050–05

ROBUST CONTROL FOR 4WS VEHICLES CONSIDERING A VARYING TIRE-ROAD FRICTION COEFFICIENT

G.-D. YIN*, N. CHEN, J.-X. WANG and J.-S. CHEN

School of Mechanical Engineering, Southeast University, Nanjing 210096, China

(Received 23 May 2008; Revised 17 December 2008)

ABSTRACT–A μ-synthesis for four-wheel steering (4WS) problems is proposed. Applying this method, model uncertainties can be taken into consideration, and a μ-synthesis robust controller is designed with optimized weighting functions to attenuate the external disturbances. In addition, an optimal controller is designed using the well-known optimal control theory. Two different versions of control laws are considered here. In evaluations of vehicle performance with the robust controller, the proposed controller performs adequately with different maneuvers (i.e., J-turn and Fishhook) and on different road conditions (i.e., icy, wet, and dry). The numerical simulation shows that the designed μ-synthesis robust controller can improve the performance of a closed-loop 4WS vehicle, and this controller has good maneuverability, sufficiently robust stability, and good performance robustness against serious disturbances.

KEY WORDS : Four-wheel steering, Optimal control, Robust control, μ-synthesis

1. INTRODUCTION

Many researchers in the last decade have reported that the four-wheel steering (4WS) technique is one of the most effective methods of active chassis control, and can considerably enhance vehicle stability and maneuverability. A large number of studies have been done on various control strategies for 4WS vehicles since the first 4WS system was reported (Young and Kim., 1995; El Hajjaji *et al*., 2005).

It is well known that vehicle maneuvering containing various uncertainties is a highly nonlinear and complex dynamic process. The parameters of a vehicle are subject to a vast range of uncertainties such as external disturbances, unmodeled dynamics, road roughness, wind gusts, load fluctuations, and braking/accelerating forces. This raises a serious robust stability problem for 4WS vehicle control. Namely, the vehicle controller has to successfully cope with these uncertainties to maintain maneuvering stability and to insure that system performance is not excessively deteriorated.

Modern robust control theory provides a powerful tool to increase robust stability and improve the performance of 4WS vehicle control against significant uncertainties. Typical robust control theory includes H_2/H_∞ synthesis (You and Chai, 1999; Lv *et al*., 2004). However, synthesis by the standard H_∞ method is relatively conservative since a system perturbation cannot be carefully distinguished with this theory, which considers only the boundary of the unmodeled dynamics. Among various approaches, the design of robust control problems can be further enhanced by μ-analysis (Packard and Doyle, 1993). Recent advances in μ-synthesis have made it possible to analyze and design a controller to deal with a dynamic system with strong uncertainties (Gao *et al*., 1995).

This paper presents the design issues of robust controllers for 4WS vehicles under a yaw rate tracking architecture by using μ-synthesis with a D-K iteration algorithm (Balas *et al*., 2001). This approach is employed to improve vehicle performance with regard to its robustness and lateral motion stability when faced with a given class of uncertainties. The vehicle yaw rate is chosen as the only feedback signal to avoid the practical difficulty of measuring the *CG* sideslip angle of the vehicle. In addition, a Linear Quadratic Regulator (LQR) controller (Zhou and Doyle, 1996), as an optimal regulator, is designed to minimize the sideslip angle. Evaluations of vehicle performance determined that the proposed controller performs adequately with different maneuvers (i.e., J-turn and Fishhook) and on different road conditions (i.e., icy, wet, and dry).

Consequently, the designed μ-synthesis controller provides a good robustness that ensures stability against parametric perturbations (such as varying cornering stiffness with different road conditions) and rejects external disturbances (such as side wind). The numerical simulation results show that the 4WS vehicle equipped with the proposed controller provides better maneuverability and driving safety. The whole control system has fine dynamic characteristics and better stability robustness and performance robustness.

2. VEHICLE MODEL

In considering the vehicle model shown in Figure 1, the

**Corresponding author.* e-mail: ygd@seu.edu.cn

4WS vehicle is assumed to be a symmetric rigid body of mass m resting on four wheels moving forward at a constant speed v. In this model, the coordinate frame is fixed on the vehicle body in the center of gravity, denoted as CG. Only lateral and yaw motions are considered, which are described by the sideslip angle β and the yaw rate r, respectively.

$$mv(\dot{\beta}+r)\cos\beta+m\dot{v}\sin\beta=F_f\cos\delta_f+F_r\cos\delta_r \tag{1}$$

$$I_z\dot{r}=L_fF_f\cos\delta_f-L_rF_r\cos\delta_r \tag{2}$$

where I_z denotes the yaw moment of inertia about its mass center z-axis, L_f and L_r are the distances from the CG to the front and rear axles, δ_f and δ_r are the steering angles of the front and rear wheels, and F_f and F_r are the lateral forces of the front and rear wheels. Because δ_f and δ_r are generally small,

$$\cos\ \delta_f\approx 1\ \text{ and }\ \cos\ \delta_r\approx 1 \tag{3}$$

The slip angles of front and rear tires are represented by α_f and α_r. If β is small and v varies slowly, α_f and α_r will be given by

$$\alpha_f=\delta_f-\beta-\frac{L_f}{v}r\ \text{ and }\ \alpha_r=\delta_r-\beta+\frac{L_r}{v}r \tag{4}$$

In general, lateral tire force is a non-linear function of slip angle. As long as the tire slip angle is small, a linear relationship between tire force and slip angle can be justified. Within the linear region, nonlinear tire characteristics can be approximated as

$$F_f=\mu K_f\alpha_f\ \text{ and }\ F_r=\mu K_r\alpha_r \tag{5}$$

where

$$K_f=K_{cf}K_{fn}\left(mg\frac{L_r}{L_f+L_r}\right),$$

$$K_r=K_{cr}K_{rn}\left(mg\frac{L_f}{L_f+L_r}\right),$$

μ is the adhesion coefficient between road surface and the tire ranging from 0.8 (dry road) to 0.25 (icy road), the cornering stiffness of the front (rear) tire is denoted by K_f (K_r), K_{fn} and K_{rn} are normalized cornering stiffnesses, and K_{cf} and K_{cr} are cornering stiffness coefficients.

Thus, the system equations of this model that govern the sideslip angle and the yaw rate are written as follows.

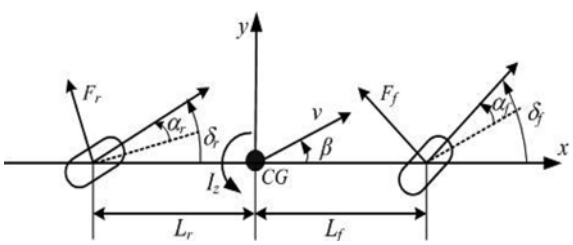

Figure 1. Half-vehicle dynamic model.

$$\begin{cases} mv\dot{\beta}=-(K_f+K_r)\mu\beta-\left\{mv+\dfrac{\mu L_fK_f-\mu L_rK_r}{v}\right\}r+\\ \mu K_f\delta_f+\mu K_r\delta_r \\ I_z\dot{r}=-(L_fK_f-L_rK_r)\mu\beta-\dfrac{L_f^2K_f+L_r^2K_r}{v}\mu r+\\ \mu L_fK_f\delta_f-\mu L_rK_r\delta_r \end{cases} \tag{6}$$

In addition, the lateral acceleration α_y at the CG is obtained by the yaw rate and the vehicle sideslip angle with the following relation:

$$\alpha_y=v(r+\dot{\beta}) \tag{7}$$

Referring to Equation (6) and (7), we obtain the state-space describing the system dynamics as

$$\begin{aligned} x&=\mathbf{A}x+\mathbf{B}u\\ y&=\mathbf{C}x+\mathbf{D}u \end{aligned} \tag{8}$$

where the state vector $x=[\beta\ r]^T$, control input vector $u=[\delta_f\ \delta_r]^T$ and the output vector $y=[\beta\ r\ a_y]^T$.

The matrices **A**, **B**, **C**, and **D** in equation (8) are given as

$$\mathbf{A}=\begin{bmatrix} -\mu\dfrac{K_f+K_r}{mv} & \mu\dfrac{-L_fK_f+L_rK_r}{mv^2}-1\\ \mu\dfrac{-L_fK_f+L_rK_r}{I_z} & -\mu\dfrac{L_f^2K_f+L_r^2K_r}{I_zv}\end{bmatrix}$$

$$\mathbf{B}=\begin{bmatrix} \dfrac{K_f}{mv}\mu & \dfrac{K_r}{mv}\mu\\ \dfrac{L_fK_f}{I_z}\mu & -\dfrac{L_rK_r}{I_z}\mu\end{bmatrix}$$

$$\mathbf{C}=\begin{bmatrix} 1 & 0\\ 0 & 1\\ -\mu\dfrac{K_f+K_r}{m} & -\mu\dfrac{-l_fK_f+l_rK_r}{mv}\end{bmatrix}$$

$$\mathbf{D}=\begin{bmatrix} 0 & 0\\ 0 & 0\\ \mu\dfrac{K_f}{m} & \mu\dfrac{K_r}{m}\end{bmatrix}$$

The key parameters of the vehicle and the tires used in this paper are summarized in Table 1.

Table 1. Parameters of the vehicle and the tires.

Parameter	Value
m (kg)	1704
L_f (m)	1.035
L_r (m)	1.655
K_f (N/rad)	35000×2
K_r (N/rad)	40000×2
I_z (kg·m^2)	3048

It is known that the linear vehicle model in Equation (8) contains plant uncertainties due to cornering stiffness, which depends on the tire characteristics and tire-road contact conditions. Thus, the coefficients in the vehicle model are generally not fixed. A robust controller has to be designed for an uncertain vehicle model.

3. ROBUST CONTROL DESIGN AND ANALYSIS

3.1. Robust Control Design and Analysis Using a μ-Approach

In vehicle control system design, it is necessary to consider changes in vehicle model parameters due to varying road conditions. In order to provide robustness against changes in the parameters, a linear feedback controller K is designed by applying μ-synthesis.

To consider the uncertainty in the vehicle running environment by μ-synthesis, we identified a nominal plant model for designing the controller. It is well known that the adhesion coefficient μ in the state-space realization matrices (**A**, **B**, **C**, **D**) is taken as a constant; that is to say, the controller design is related to a constant μ at that moment, but in practice, the adhesion coefficient always varies within a range, tracking uncertainties from the set of all possible system variations. It is always necessary to design different controller parameters corresponding to different adhesion coefficients and to perform real-time switching of the controller parameters in response to the current cornering stiffness. However, changes in the controller parameters are not smooth; thus, it is desired to have a controller parameter designed for only one adhesion coefficient that will also work well for a certain constant range.

As shown in Figure 2, the closed-loop system includes the feedback structure of the model G and controller K and elements associated with the uncertainty models and performance objectives. In the diagram, u is the control input, which denotes the rear wheel angle. Since the estimation of the sideslip angle is difficult but the yaw rate is easier to measure in practice, the yaw rate is chosen as the only feedback signal to determine the control of the system. Measurement noise is designated by n. In the figure, the front wheel angle δ_f is considered as the external disturbance signal w. The value z represents the performance output, which is the sideslip angle, which is usually minimized to approach zero in the four-wheel steering control system.

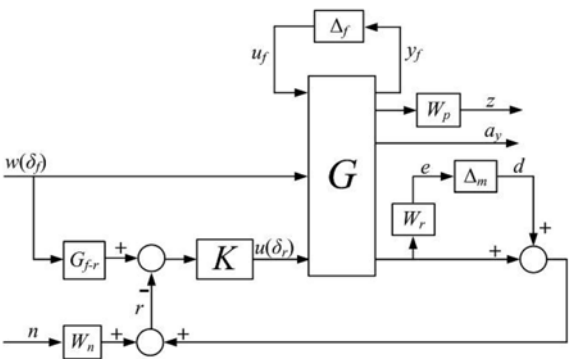

Figure 2. 4WS closed-loop interconnection structure.

In this system, the desired yaw rate G_{f-r} is selected as (Nagai *et al*., 1997; An *et al*., 2008)

$$G_{f-r}(s)=\frac{s/300+3.75}{s/10+1} \tag{9}$$

where G_{f-r} corresponds to a yaw rate of vehicle response, which is agile and without much overshoot.

To deal with system perturbation, the weighting function is a key issue in the μ-synthesis design process. The weighting matrices, which characterize the input/output signals of the control system, have to be formulated appropriately. Since the robust controller has to provide a desired degree of stability and performance robustness, it is necessary to translate the design specifications into frequency-dependent weighting functions.

The parametric uncertainties of the mass, velocity, and adhesion coefficient are represented by the Δ_f block, whose input and output are y_f and u_f. Moreover, the transfer function Δ_f block is stable and norm-bounded, $\|\Delta_f\|_\infty<1$. The unmodeled dynamics are represented by W_r and Ä$_m$. It is assumed that the transfer function W_r is known and that it reflects the uncertainty in the model. The transfer function Δ_m is assumed to be stable and unknown with the norm condition $\|\Delta_m\|_\infty<1$.

The high-pass frequency weightings can be described as

$$W_r(s)=1.75\frac{s+40}{s+200} \tag{10}$$

At any frequency ω, the magnitude of $|W_r(j\omega)|$ can be interpreted as the percentage of model uncertainty at that frequency. Therefore, this particular weight implies that the model error can potentially be about 35% at low frequency and up to 100% at high frequency.

The weighting function W_p represents the performance outputs, which are related to the components of z. Subsequently, the performance weighting function is used to define design specification. The inverse of the performance weight indicates the fraction of the external disturbances to be rejected at the output, i.e., the amount of steady state tracking due to external input to allow. $W_p(j\omega)$ for the sideslip angle are the weights specifying system performance. The upper bound on $|1/W_r(j\omega)|$ is the weight for the tolerable maximum angle β; the weight is assumed to be constant over all frequencies and is set to

$$W_p=\frac{0.3s+0.5}{s+0.01} \tag{11}$$

The corresponding steady-state control error is less than 0.01/0.5=2%.

The input of the perturbation is denoted as e, and d is its output. The weighting function W_n represents the impact of the different frequency domain in terms of sensor noise n.

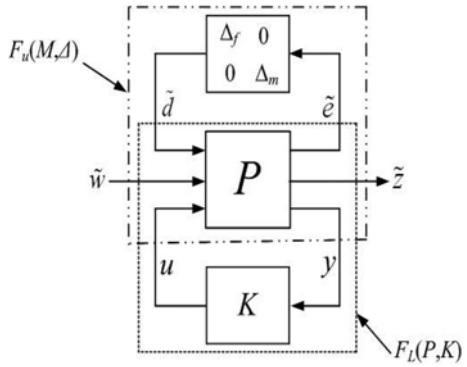

Figure 3. P-K structure with uncertainty.

To account for the inability to sense system outputs without noise, all measurement signals will always be corrupted by frequency-dependent noise. The noise-varying frequency should be suppressed. In this study, the noise occurs at a high frequency. Therefore, it has to be weighted by high-pass characteristics. The weighting W_n(s) is given by

$$W_n=\frac{0.006(s+1)}{500s+1} \tag{12}$$

where the upper bound of $|1/W_n(j\omega)|$ represents the maximal expected noise gain.

Necessary and sufficient conditions for robust stability and robust performance can be formulated in terms of the structured singular value denoted as μ (Packard and Doyle, 1993; Zhou and Doyle, 1996). At this point, the design setup in Figure 2 should be formalized as a standard design problem. In order to analyze the performance and robustness requirements, the closed-loop system, which is illustrated in Figure 3, is expressed by using the feedback effect $u=Ky$.

It should be noted that the system P consists of recognizing three pairs of input/output variables. The complete vehicle model for the control system is described by

$$\begin{bmatrix}\tilde{e}\\ \tilde{z}\\ y\end{bmatrix}=\underbrace{\begin{bmatrix}P_{11} & P_{12} & P_{13}\\ P_{21} & P_{22} & P_{23}\\ P_{31} & P_{32} & P_{33}\end{bmatrix}}_{P(s)}\begin{bmatrix}\tilde{d}\\ w\\ u\end{bmatrix} \tag{13}$$

$$\tilde{d}=\Delta\tilde{e} \tag{14}$$

where $\tilde{d}=[u_f\ \ d]^T$, $\tilde{e}=[y_f\ \ e]^T$, $\tilde{w}=[w\ \ n]^T$, $\tilde{z}=z$.

The system P augmented with weighting functions can be re-partitioned as described in Equation (13). For the problem, the controller K can be combined with P via a lower linear fractional transformation (LFT) to yield the transfer function matrix M:

$$M(s)=F_L(P(s),K(s))=\begin{bmatrix}P_{11} & P_{12}\\ P_{21} & P_{22}\end{bmatrix}+ P_{13}K(I-P_{33}K)^{-1}\begin{bmatrix}P_{31} & P_{32}\end{bmatrix}\begin{bmatrix}M_{11} & M_{12}\\ M_{21} & M_{22}\end{bmatrix} \tag{15}$$

which is actually obtained by substituting $u=Ky$ into Equation (13).

The LFT paradigm can be used to describe and analyze the uncertain vehicle system, where M corresponds to what is assumed to be the constant in the control system and Δ is the block diagonal matrix. The matrix M is then partitioned as

$$\begin{bmatrix}\tilde{e}\\ \tilde{z}\end{bmatrix}=\underbrace{\begin{bmatrix}M_{11} & M_{12}\\ M_{21} & M_{22}\end{bmatrix}}_{M(s)}\begin{bmatrix}\tilde{d}\\ w\end{bmatrix} \tag{16}$$

Moreover, the upper LFT connects w and z, which is obtained by combining Equation (14) with Equation (16) and expressed as

$$\tilde{z}=F_u(M,\Delta)w=[M_{22}+M_{21}\Delta(I-M_{11}\Delta)^{-1}M_{12}]w \tag{17}$$

where $F_u(M, \Delta)$ is the upper LFT. The robust performance of the closed-loop system with nominal plant perturbation is equivalent to $\|F_u(M, \Delta)\|_\infty<1$.

The goal of the μ-synthesis is to minimize the peak value $\mu_\Delta(\cdot)$ of the closed loop transfer function $F_L(P, K)$ over all stabilizing controllers K. The formula is as follows:

$$\min_{\substack{K\\ \text{stabilizing}}}\sup_{\omega\in R}\mu_\Delta\left[F_L(P,K)(j\omega)\right] \tag{18}$$

In this formula, the block structure Δ is defined in the following form:

$$\Delta:=\left\{\begin{bmatrix}\Delta_f & \\ & \Delta_m\end{bmatrix}\middle|\Delta_f\in C^{2\times 2},\Delta_m\in C^{2\times 1}\right\}\subset C^{4\times 3} \tag{19}$$

The first block of this structured set with input y_f and output u_f corresponds to the scalar-block uncertainty Δ_f, which is used to model the uncertainty. The second block, Δ_m, is a fictitious uncertainty block with input e and output d. This block is applied to incorporate the H_∞ performance objective of the weighted output sensitivity transfer function into the μ-framework.

Subsequently, the structured singular value (SSV) (μ) of a complex matrix M is defined with respect to a block structure Δ as follows:

$$\mu_\Delta(M)=\left[\min\left\{\sigma(\Delta):\Delta\in\tilde{\Delta},\det(I-M\Delta)=0\right\}\right]^{-1} \tag{20}$$

unless no $\Delta\in\tilde{\Delta}$ makes I-$M\Delta$ singular, in which case, $\mu_\Delta(M)=0$. Thus, $1/\mu_\Delta(M)$ is the 'size' of the smallest perturbation Δ, measured by its maximum singular value, which makes $\det(I-M\Delta)=0$. It has been shown that the computation of μ is an NP hard problem. However, tight upper and lower bounds for μ may be effectively computed for the perturbation sets.

At present, no direct method is practical for synthesizing a μ optimal controller; however, the D-K iteration that combines μ-analysis with μ-synthesis yields good results. For a constant matrix M and an uncertainty structure Δ, the

upper bound of $\mu_\Delta(M)$ is an optimally scaled maximum singular value:

$$\mu_\Delta(M) \le \inf_{D\in\mathbf{D}_\Delta} \bar{\sigma}(DMD^{-1}) \tag{21}$$

where $\mathbf{D}_\Delta$ is the set of matrices with the property that $D\Delta=\Delta D$ for every $D \in \mathbf{D}_\Delta$, $\Delta \in \Delta$.

Using this upper bound, the optimization is reformulated as

$$\min_{\substack{K \\ \text{stabilizing}}} \max_{\omega} \min_{D_\omega \in \mathbf{D}_\Delta} \sigma\left[D_\omega F_L(P,K)(j\omega)D_\omega^{-1}\right] \tag{22}$$

where D_ω is selected from the set of scaling **D** independently of every ω. The optimization problem can be solved in an iterative way using K and D, called D-K iteration. It is performed with a two-parameter minimization in a sequential way, first minimizing over K with D_ω fixed, then minimizing pointwise over D_ω with K fixed, etc., although the joint optimization of D and K is not convex and global convergence is not guaranteed.

3.2. Optimal Control Design

The goal of linear quadratic optimization control is to seek an optimization controller signal $u(t)$ that minimizes the following performance index J with reference to the system described by Equation (8):

$$J = \int_0^\infty (x^T Q x + u^T R u)dt \tag{23}$$

Here, the state that weighting coefficient $Q \ge 0$, and the input weighting coefficient $R>0$. (**A**,**B**) is assumed to be controllable, and (**A**,**C**) is assumed to be observable. The control input u that minimizes Equation (23) is $u=-K_{op}x$, where K_{op} is called an optimal feedback coefficient matrix given by $K_{op}=R^{-1}B^TP$. Here, P, which is a positive definite matrix, is the solution of the following Riccati matrix equation:

$$-P\mathbf{A}-\mathbf{A}^TP+P\mathbf{B}R^{-1}\mathbf{B}^TP-Q=0 \tag{24}$$

Therefore, to regulate the dynamics of the vehicle model, the controller may attempt to minimize the sideslip angle to improve the vehicle handling stability performance. By trial and error, Q and R take the following values:

$$Q=\begin{bmatrix} 100 & 0 \\ 0 & 1 \end{bmatrix} \quad R=\begin{bmatrix} 100 & 0 \\ 0 & 1 \end{bmatrix}$$

4. NUMERICAL SIMULATION RESULTS

4.1. Comparison of Robust and Optimal Control Simulation

In this section, the dynamic performances of both versions of the controller will be compared in order to validate the approximation put forward. In what follows, the 4WS robust controllers are evaluated in the time domain using μ-Toolbox (Balas *et al*., 2001). As shown in the μ design procedure with the D-K iteration, a robust controller is synthesized and designed for the 4WS vehicle at a velocity of 30 m/s. The results of the iterations are summarized in Table 2.

Table 2. Summary of D-K iteration.

Iteration	#1	#2	#3
Controller order	8	12	14
Total D-scale order	0	4	2
Gamma achieved	3.134	1.486	0.992
Peak μ-value	2.308	1.192	0.865

To achieve the desired performance and to deal with the uncertainty for the considered vehicle, a set of frequency-dependent weightings have to be included; thus, the order of the generalized 4WS control system is increased, resulting in a high-order controller. It is difficult to implement a high-order controller because the controller is normally ill-conditioned. By adopting a balanced model reduction via a truncation method (Safonov and Chiang, 1989), the 14-order controller obtained by the above iteration can be reduced to a 3-order controller. In reality, the controller has to be discretized because it is implemented by a digital computer. By using bilinear transformation, a continuous reduced-order controller K(s) can be discretized as

$$K_T(z)=\frac{-22.87z^2+45.52z-22.58}{z^3-1.959z^2+0.96z-001446}$$

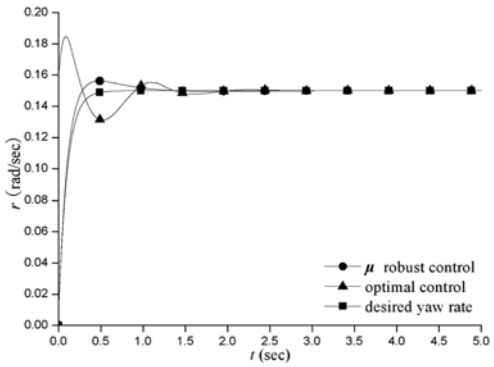

Figure 4(a). Yaw rate response for robust and optimal control laws.

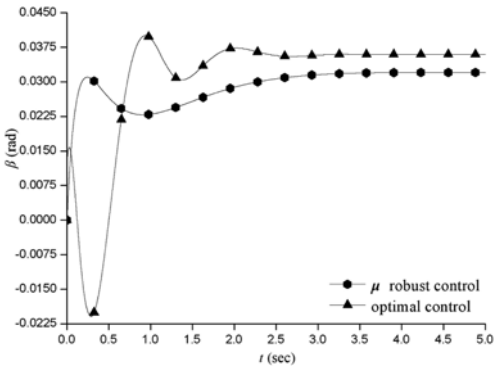

Figure 4(b). Sideslip angle response for robust and optimal control laws.

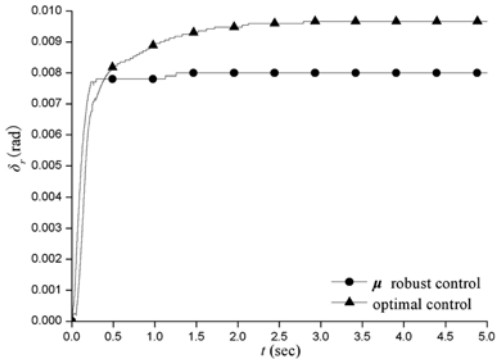

Figure 4(c). Rear angle response for robust and optimal control laws.

where T is the sampling time interval; that is, T=1/1024 sec in our simulation.

Figure 4 illustrates the simulation results of the transient response to the steering wheel angle input, which changes from 0 to 35 deg (gear ratio=15). Thus, the given front wheel steering angle δ_f is 0.04 rad, approximately equivalent to 2.29 deg.

Results obtained from the computer simulation indicate that the vehicle with the robust controller has superior performance compared to one with the optimal control. Figure 4(a) illustrates that the steady state values of the yaw rate of two controllers are almost equal to that of the desired yaw rate. However, the yaw rate response of the robust controller is more rapid than that of the optimal controller, and the peak value of the robust controller is lower than that of the optimal controller. This means that lower sensitivity of the steering system is achieved at high speed with the robust controller. Furthermore, Figure 4(b) indicates that reduction in the vehicle sideslip angle is an important safety criterion, which could certainly be further reduced in the robust controlled vehicle. Figure 4(c) shows the turning of the rear steering angle as control input is maintained as the front steering angle.

Overall, the comparison of robust and optimal controls for improving vehicle performance shows that the robust controller can certainly improve vehicle handling compared to the performance of the optimal controller. The following simulation was performed to further validate the superiority of the robust controller.

4.2. μ Robust Control Simulation

From the evaluation of the performance of vehicles with the robust controller, the proposed controller performs adequately with different maneuvers and on different road conditions (dry road μ=0.8, wet road μ=0.4, icy road μ=0.25). The primary maneuvers are variations of J-turn and fishhook maneuvers. The J-turn maneuver simulates vehicle behavior under sudden turns onto a sharp ramp. In this maneuver, at the start, the vehicle is moving in a straight line. Because the front wheel steering angle is commonly proportional to the steering wheel angle controlled by driver,

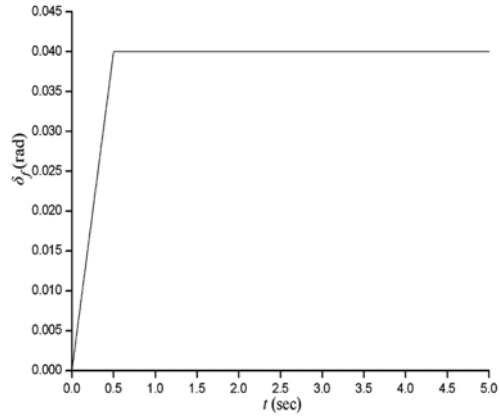

Figure 5(a). J-turn maneuver.

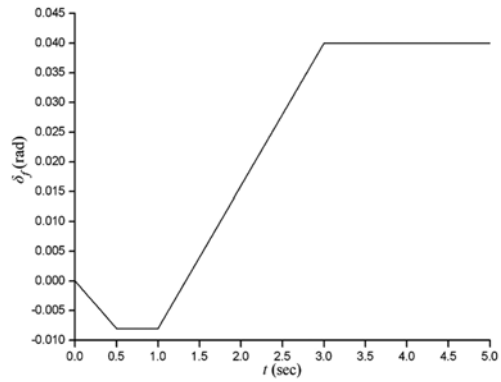

Figure 5(b). Fishhook maneuver.

the front wheel steering angle is taken as the input signal. At time 0 s, the driver turns the steering wheel from 0 to 0.6 rad (the front wheel steering angle changing by 0.04 rad) within 0.5 s. Figure 5(a) shows the front wheel steering angle as a function of time. The fishhook maneuver attempts to induce two-wheel lift-off by suddenly making a drastic turn and then turning back even further in the opposite direction. As shown in Figure 5(b), the driver turns the steering wheel from 0 to approximately 0.12 rad during the first 0.5 s. After maintaining the steering angle for 0.5 s, the driver turns the steering wheel in the opposite direction to

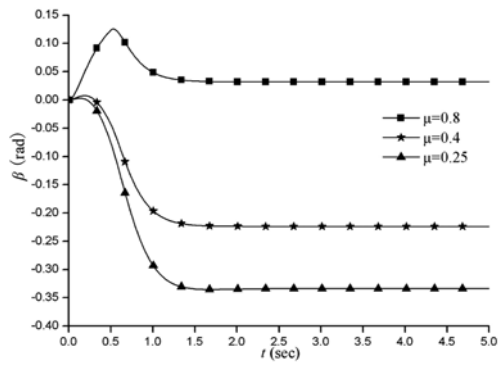

Figure 6. Sideslip angle response under the J-turn maneuver.

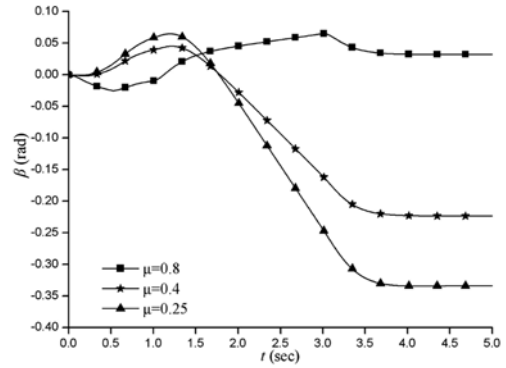

Figure 7. Sideslip angle response under the Fishhook maneuver.

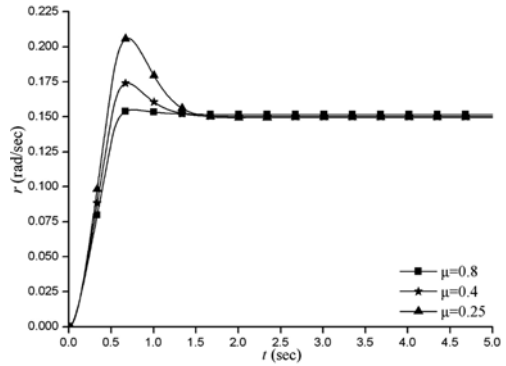

Figure 8. Yaw rate response under the J-turn maneuver.

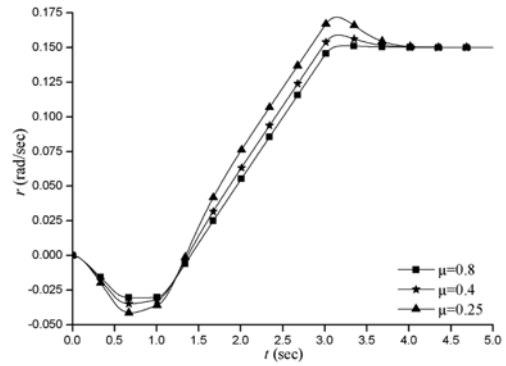

Figure 9. Yaw rate response under the Fishhook maneuver.

0.6 rad within 2 s and maintains it at that position for the remainder of the maneuver.

Figure 6 through Figure 9 show the time responses of the vehicle with yaw rate and sideslip angle under J-turn and Fishhook maneuvers, respectively. In Figure 6 and Figure 7, the sideslip angle steady state gain under dry road conditions is approximately zero. It can be seen that the sideslip angle steady state gain is less than zero under wet and icy road conditions, which shows that the sideslip and running directions are opposite of each other when the vehicle runs at low adhesion coefficients. Moreover, the same trends are seen with the running direction under the two different maneuvers.

As shown in Figure 8 and Figure 9, the yaw rate gains are equal to the desired yaw rate gain at steady state for both maneuvers. It can be seen that the settling process is rapid; during the transient response, every yaw rate has little overshoot under different road conditions, which proves that the designed robust controller is not sensitive to system disturbance.

From Figure 6 through Figure 9, we determine that the lateral acceleration has a maximum peak value when μ= 0.25, and the peak values do not exceed 0.4 g. It is also shown that the 4WS vehicle equipped with the μ-synthesis controller maintains good lateral acceleration while responding to rather serious system perturbations.

5. CONCLUSIONS

In this paper, a robust μ-method has been applied to a four-wheel steering system design. Since a vehicle runs on different road conditions, vehicle system uncertainty always exists and must be dealt with carefully. The proposed controller performs adequately with different maneuvers (i.e., J-turn and Fishhook) and on different road conditions (i.e., icy, wet, and dry). A μ-synthesis robust controller with optimized weighting functions for the considered structure uncertainties is chosen to resist the disturbances. Therefore, the 4WS vehicle with a μ-synthesis robust controller has good maneuverability, sufficiently robust stability, and good performance robustness against serious disturbance.

ACKNOWLEDGEMENT–This work was supported by National Natural Science Foundation of China Fund (No. 50975047), Southeast University Technology Foundation (No. KJ2009346).

REFERENCES

An, S.-J., Yi, K., Jung, G., Lee, K. I. and Kim, Y. W. (2008). Desired yaw rate and steering control method during cornering for a six-wheeled vehicle. *Int. J. Automotive Technology* **9**, **2**, 173–181.

Balas, G. J., Doyle, J. C., Glover, K., Packard, A., Smith, R. (2001). *μ-Analysis and Synthesis Toolbox User'S Guide*. The Math Works.

El Hajjaji, A., Ciocan, A. and Hamad, D. (2005). Four wheel steering control by fuzzy approach. *J. Intelligent and Robotic Systems*: *Theory and Applications* **41**, **2/3**, 141–156.

Gao, X., McVey, B. D. and Tokar, R. L. (1995). Robust controller design of four wheel steering systems using μ synthesis techniques. *Proc. 34th IEEE Conf. Decision and Control*, **1**, 875–882.

Lv, H.-M., Chen, N. and Li, P. (2004) Multi-objective *H* optimal control for four-wheel steering vehicle based on a yaw rate tracking. *IMechE Part D, J. Automobile Engineering* **218**, **10**, 1117–1124.

Nagai, M., Hirano, Y. and Yamanaka, S. (1997). Integrated control of active rear wheel steering and direct yaw

moment control. *Vehicle System Dynamics* **27**, **5**, 357–370.

Packard, A. and Doyle, J. (1993) Complex structured singular value. *Automatica* **29**, **1**, 71–109.

Safonov, M. G. and Chiang, R. Y. (1989). Schur method for balanced-truncation model reduction. *IEEE Trans. Automat. Contr.* **34**, **7**, 729–733.

Young, H. C. and KIM, J. (1995). Design of optimal four-wheel steering system. *Vehicle System Dynamics* **24**, **9**, 661–682.

You, S.-S. and Chai, Y.-H. (1999). Multi-objective control synthesis: An application to 4WS passenger vehicles. *Mechatronics* **9**, **4**, 363–390.

Zhou, K. and Doyle, J. C. (1996). *Robust and Optimal Control*. Prentice Hall. New Jersey.